Original Research Paper

Measurement and correlation study of silymarin solubility in supercritical carbon dioxide with and without a cosolvent using semi-empirical models and back-propagation artificial neural networks

Gang Yang [a,1], Zhe Li [a,1], Qun Shao [b], Nianping Feng [a,*]

[a] Department of Pharmaceutical Sciences, Shanghai University of Traditional Chinese Medicine, Shanghai, 201203, China

[b] Open Innovation, University of Bradford, West Yorkshire, BD7 1DP, UK

ARTICLE INFO

ABSTRACT

The solubility data of compounds in supercritical fluids and the correlation between the experimental solubility data and predicted solubility data are crucial to the development of supercritical technologies. In the present work, the solubility data of silymarin (SM) in both pure supercritical carbon dioxide ($SCCO_2$) and $SCCO_2$ with added cosolvent was measured at temperatures ranging from 308 to 338 K and pressures from 8 to 22 MPa. The experimental data were fit with three semi-empirical density-based models (Chrastil, Bartle and Mendez-Santiago and Teja models) and a back-propagation artificial neural networks (BPANN) model. Interaction parameters for the models were obtained and the percentage of average absolute relative deviation (AARD%) in each calculation was determined. The correlation results were in good agreement with the experimental data. A comparison among the four models revealed that the experimental solubility data were more fit with the BPANN model with AARDs ranging from 1.14% to 2.15% for silymarin in pure $SCCO_2$ and with added cosolvent. The results provide fundamental data for designing the extraction of SM or the preparation of its particle using $SCCO_2$ techniques.

* Corresponding author. Shanghai University of Traditional Chinese Medicine, Shanghai, 201203, China. Tel.: +86 21 5132 2198.
E-mail address: npfeng@hotmail.com (N. Feng).
Peer review under responsibility of Shenyang Pharmaceutical University.
[1] These two authors contributed equally to this study.

1.　Introduction

In recent years, supercritical fluids (SCF) have been widely applied in the fields of pharmaceuticals, food nutrition, and industrial materials [1–3] owing to their non-toxic, non-flammable, non-explosive and recyclable properties. On the other hand, working with SCF requires high-pressure processes which imply high investment costs for the machinery and the training of skilled staff [4]. For the application of SCF in extraction, reaction, waterless dyeing processes and particle preparation [5–8], the solubility of compounds in SCF is a key parameter in process design. Since experimentally acquiring solubility data is time consuming and laborious, understanding and ultimately predicting the solubility of related compounds are very helpful in supercritical process design or election parameter [9]. Supercritical carbon dioxide ($SCCO_2$) is the most widely used SCF for its temperate critical conditions, low cost, quick diffusion, and excellent dissolving capacity [10]. There are several studies on solubility data of substances in $SCCO_2$ [11–14]. However, there have been only a few studies on the solubility of flavonoids [15,16], and no solubility data for silymarin has been analyzed thus far.

Silymarin (SM), a hepatoprotective agent obtained from the herb *Silybum marianum* (L.), is widely used in the treatment of liver diseases such as cirrhosis, hepatitis, and fatty infiltration due to alcohol and toxins [17]. A mixture of flavonolignan isomers, namely silybin, isosilybin, silydianin, and silychristin, collectively constitute SM. Among these isomers, silybin is the major component of SM, representing approximately 60–70%, and is responsible for its pharmacological activity [18–21]. Extraction of SM using $SCCO_2$ has many advantages, such as lower extraction temperature, shorter extraction time, and no remains of toxic solvents [22,23]. Moreover, $SCCO_2$ can be utilized to produce SM nanoparticles, solid dispersion and liposomes that may improve the bioavailability of SM, in which the supercritical antisolvent (SAS) and solution-enhanced dispersion by supercritical fluids (SEDS) methods were often utilized [24–26]. Thus, the solubility of SM in $SCCO_2$ is important for all of these processes. Among the factors responsible for the limited acceptance of SCF technologies, the insufficiency of supercritical solubility data has been frequently cited.

However, the measurement of equilibrium solubilities of solids in SCF at different temperatures and pressures is experimentally expensive and time consuming; hence, the modeling of the solubilities is essential. The models classically used to fit with the solubility of solid solutes are semi-empirical equations such as Chrastil [27], Bartle [28], Mendez-Santiago and Teja (MST) [29] models. Semi-empirical models only need independent variables like pressure, temperature and density of SCF instead of solid properties [30,31]. They are based on simple error minimization. Nowadays, application of BPANN has been considered a promising tool because of their simplicity toward simulation, prediction and modeling. One of the characteristics of modeling based on BPANN is that it does not require the mathematical description of the phenomena involved in the process, and might therefore prove useful in simulating and up-scaling complex systems. So, it is preferable to use a nonparametric technique such as a neural network model to make reliable prediction of silymarin solubility in the $SCCO_2$ and co-solvent system [32].

The purpose of this study is to provide fundamental data for the extraction and particle preparation process of SM using the $SCCO_2$ technology, and to find a way of predicting the solubility of SM in $SCCO_2$. During our research, the equilibrium solubility of SM was measured in $SCCO_2$ with a static method in the pressure range of 8 to 22 MPa and at temperatures equal to 308, 318, 328 and 338 K. The influence of ethanol, acetone and dichloromethane as cosolvents on solubility was also investigated. Finally, three semi-empirical models (Chrastil, Bartle, and Mendez-Santiago and Teja models) and a back-propagation artificial neural networks (BPANN) model were applied to fit with the experimental solubility data and predict the solubility of SM in $SCCO_2$ at different conditions

2.　Material and methods

2.1.　Materials

Silymarin and oridonin were purchased from Dalian Meilun Biotech Co., Ltd. (Dalian, China). CO_2 with a purity of 99.99% was obtained from SJTU chemical store (Shanghai, China). Ethanol, acetone and dichloromethane were purchased from Shanghai Lingfeng Chemical Reagent Co., Ltd. (Shanghai, China).

2.2.　Apparatus and procedure

The solubility of SM in $SCCO_2$ was measured by a semi-dynamic technique, as shown by the schematic (Fig. 1). Solubility measurements were taken in the pressure range of 8 to 22 MPa at temperatures of 308 to 338 K. A certain amount of SM powder was preloaded in the saturation cell and the procedure of solubility measurement was as follows: Before the experiment, CO_2 was delivered by a high pressure piston pump into the saturation cell for air removal by adjusting the pressure relief valve V_R. The high pressure CO_2 then passed into the system, heated and kept at the desired temperature with a temperature sensor. After the desired conditions were achieved, the valves V_R and V_1 were closed. The $SCCO_2$ was made to circulate in the system by the circulating pump. Based on pre-experimental results, the circulating time was set for 90 min. When the system reached equilibrium, the valves V_2 and V_C at the inlet and outlet of the 50 ml U-sample collector were closed, and the certain amount of $SCCO_2$ with dissolved solute was sealed inside. The amount of $SCCO_2$ can be calculated using the CO_2 density corresponding to the operating conditions and the inner volume of the collector. Finally, the U-sample collector was taken down, cooled, and depressurized very slowly by releasing the CO_2 into a 100 ml beaker containing 20 ml of ethanol, to precipitate the dissolved SM precipitated inside the U-sample collector. The U-sample collector was then washed with ethanol more than three times, and the washing solvent was combined with the solution of the beaker. All experiments were performed in triplicate.

The procedure of measuring the SM solubility in $SCCO_2$ with a cosolvent at a mole fraction of 0.02 was similar, except that at the beginning, a calculated amount of solvent was injected into the system in advance.
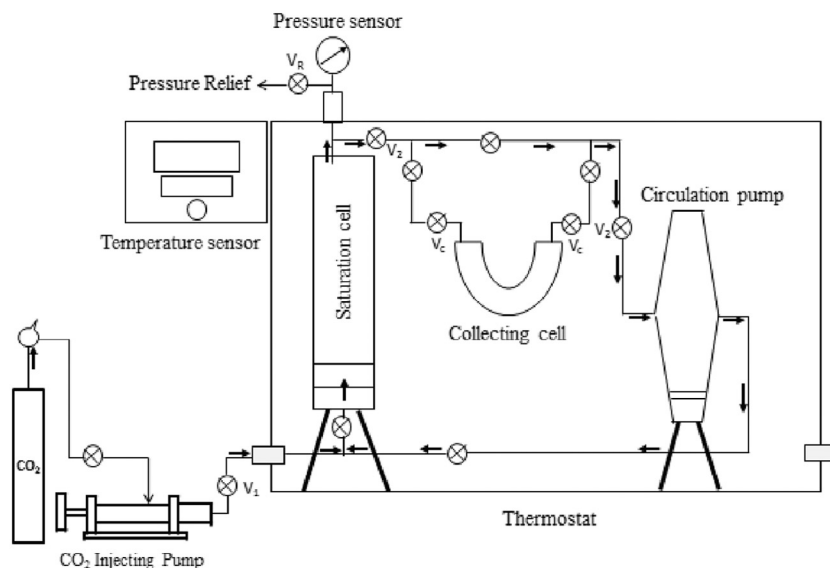
Fig. 1 – Schematic diagram of the experimental apparatus.

2.3. Analytical method

The obtained solution was analyzed by high-performance liquid chromatography (HPLC). The content of SM (based on silybin) was determined using a LC-2010A HT HPLC system (Shimadzu, Tyoto, Japan) with an Agilent Eclipse XDB-C18 column (5 ìm, 4.6 × 250 mm) (Agilent, Shanghai, China). The mobile phase consisted of methanol and pure water (46:54, v/v) at a flow rate of 0.8 ml/min. The effluent was monitored at 288 nm. Each data point was measured at least three times and the average value was adopted. The SM solubility in $SCCO_2$ with or without a cosolvent was defined as the mole ratio of SM to CO_2 in the U-sample collector. The mole amount of CO_2 was calculated based on the inner volume of U-sample collector and the density of CO_2 corresponding to the operating conditions, which was obtained from the National Institute of Standards and Technology (NIST) fluid property database.

2.4. Correlation models

In this work, Chrastil, Bartle, Mendez-Santiago and Teja (MST), and BPANN models were used to fit with the experimental solubility data.

Chrastil is based on the association theory of formation of a solvate complex, which was assumed to be in equilibrium with the supercritical fluid. Mathematically, it is given by the expression.

$$\ln y = A_1 + A_2 \ln \rho + \frac{A_3}{T}$$

Where y is the solubility of solute, ρ is density of SCF, T is temperature, A_1 and A_3 are the regression coefficient and A_2 is association number.

The next model proposed by Bartle and co-workers fit with the solubility using the following equation.

$$\ln\left(\frac{yP}{P_C}\right) = A_1 + A_2(\rho - \rho_C) + \frac{A_3}{T}$$

Where y is the solubility of solute, ρ is density of SCF, ρ_c is 700 kg/m^3. P is the pressure, P_c is assumed as a standard pressure of 0.1 MPa. T is temperature, A_1 and A_3 are the regression coefficient and A_2 is association number.

Another important semi-empirical model is MST model which derived a relation between the enhancement factor and the density using the theory of dilute solutions given by the following expression.

$$T\ln(y\rho) = A_1 + A_2\rho + A_3T$$

Where y is the solubility of solute, ρ is density of SCF, T is temperature, A_1 and A_3 are the regression coefficient and A_2 is association number.

BPANN is a type of supervised network, and has been generally accepted for its excellent capability to train rapidly on sparse data sets. It has three layers. The number of neurons in the first layer (input layer) is equal to the number of inputs and the number of neurons in the third layer is equal to the number of outputs (output layer). The number of neurons in the second layer (hidden layer) is equal to or more than the number of training data sets. The data are scaled using a scaling function before it is used for training. During the training of BPANN, a neuron for each training pattern is assigned in the pattern layer. The weights between the pattern layer neurons and the input layer neurons are equal to the inputs of the training patterns. The outputs of the training patterns are assigned as the weights between the pattern layer neurons and thesummation layer neurons. Fig. 2 presents the BPANN block diagram.
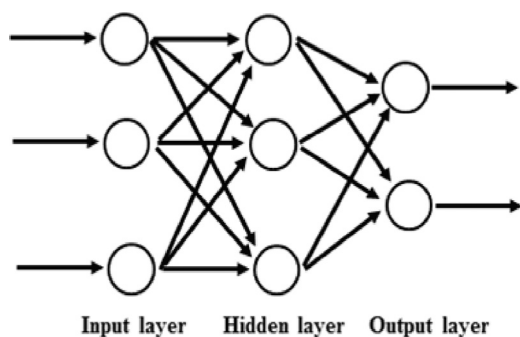
Fig. 2 – Representation of BPANN. (Semi-empirical models and BPANN were designed by softwares of 1stopt and MATLAB, respectively.)

Fig. 3 – Comparison of solubility data of oridonin in $SCCO_2$.

3. Results and discussion

3.1. Experimental solubility equilibrium data

To start with, the reliability and efficiency of the solubility measurement apparatus and the procedures were verified by measuring the solubility of oridonin in $SCCO_2$ at 308 K and 328 K and comparing with literature data [33]. The results are shown in Table 1 and Fig. 3, where satisfactory agreement between various measurements can be observed.

Isothermal solubility for the system in pure $SCCO_2$ over the pressure range of 8 to 22 MPa and temperature range of 308 to 338 K are tabulated in Table 2 and solubility of SM in $SCCO_2$ with a cosolvent (ethanol, acetone or dichloromethane) at a mole fraction of 0.02 under the same conditions are shown in Table 3. Each reported data point is the average of at least three replicate measurements with relative standard deviations of less than 2.6 %. The solubility data of SM with and without a solvent in $SCCO_2$ shows the same trend when it is plotted as a function of pressure. The solubility increases with the increase of pressure at a constant temperature. This can be explained by the increase of solvent density attributed to

pressure growth along an isotherm as well as specific interaction between dissolved substances and solvent molecules in elevated pressure. Increase of carbon dioxide density will also increase the polarity of its molecules [34].

Crossover points have been observed for all groups as shown in Fig. 4. The crossover pressure regions of SM without a solvent and with ethanol, acetone and dichloromethane are from 12.5

Table 1 – Solubility of oridonin in pure $SCCO_2$ at temperatures of (308 and 328) K and pressures from (9 to 17) MPa.

T^a (K)	P (MPa)	P^b(g/L)	Oridonin $y.10^6$
308	9	662.13	0.57
	11	743.95	1.62
	13	785.70	3.29
	15	815.06	5.41
	17	838.09	7.60
328	9	255.54	0.36
	11	414.90	0.60
	13	571.33	0.77
	15	653.50	1.32
	17	703.82	1.98

[a] Standard uncertainties u are the following: u (T) = 0.1 K, u (P) = 0.2 MPa, u (y) = 2.3 %.
[b] ρ is the density of pure CO_2 obtained from the National Institute of Standards and Technology (NIST) fluid property database.
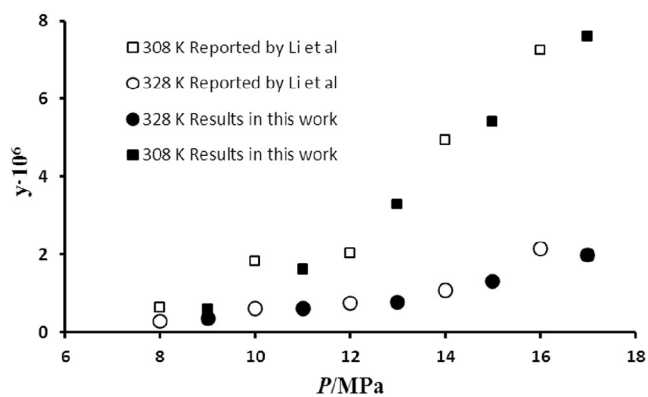
Table 2 – Solubility of SM in pure $SCCO_2$ at temperatures of (308, 318, 328 and 338) K and pressures from (8 to 22) MPa.

T^a (K)	P (MPa)	P^b (g/L)	SM $y.10^5$
308	8	419.09	1.32
	10	712.81	1.41
	12	767.07	1.53
	14	801.41	1.69
	16	827.17	1.93
	18	848.04	2.11
	20	865.72	2.34
	22	881.15	2.75
318	8	241.05	1.02
	10	498.25	1.37
	12	657.74	1.58
	14	720.47	1.87
	16	759.98	2.34
	18	789.24	2.65
	20	812.69	3.20
	22	832.36	4.07
328	8	203.64	0.61
	10	325.07	0.92
	12	504.51	1.41
	14	618.45	2.12
	16	681.12	2.75
	18	723.08	3.41
	20	754.61	4.24
	22	779.93	5.38
338	8	181.84	0.27
	10	265.85	0.59
	12	382.87	1.32
	14	505.73	2.51
	16	592.39	3.77
	18	650.05	5.04
	20	691.71	6.41
	22	724.03	8.01

Table 3 – Solubility of SM in SCCO$_2$ with a cosolvent (ethanol, acetone or dichloromethane) at a mole fraction of 0.02 at temperatures of (308, 318, 328 and 338) K and pressures from (8 to 22) MPa.

T^a (K)	P(MPa)	SM + ethanol + CO$_2$ y.10^5	SM + acetone + CO$_2$ y.10^5	SM + dichloromethane + CO$_2$ y.10^5
308	8	7.12	10.75	5.78
	10	7.21	12.33	6.12
	12	7.76	15.16	6.78
	14	8.45	19.32	7.61
	16	9.33	25.88	8.59
	18	10.87	33.11	10.01
	20	13.07	44.08	12.55
	22	18.88	54.81	14.08
318	8	6.71	8.97	4.37
	10	7.23	12.02	5.08
	12	8.55	16.11	6.11
	14	10.92	21.74	7.92
	16	14.65	31.65	9.29
	18	17.71	42.17	12.9
	20	22.11	56.14	16.33
	22	30.54	68.90	18.76
328	8	4.45	7.66	3.12
	10	6.78	10.13	4.37
	12	9.66	17.65	5.86
	14	13.12	26.72	7.42
	16	18.46	37.19	10.16
	18	24.77	50.08	15.67
	20	33.14	65.72	21.71
	22	41.99	83.24	27.18
338	8	3.89	5.17	2.99
	10	5.99	8.22	4.87
	12	10.12	15.51	6.81
	14	16.98	26.40	11.14
	16	24.11	41.73	16.32
	18	34.24	60.06	23.82
	20	47.76	80.06	31.19
	22	60.12	101.37	40.33

^{a} Standard uncertainties u are the following: u (T) = 0.1 K, u (P) = 0.2 MPa, u (y) = 1.4 %.

to 12.8 MPa, 11.4 to 11.7 MPa, 11.8 to 12.3 MPa and 13.9 to 14.2 MPa, respectively. The crossover phenomena may be attributed to competition between the solute's vapor pressure and the solvent's density, which have opposing temperature dependences. Below the crossover pressure region, the effect of density, which is sensitive to the solute's vapor pressure, is dominant so that the solute is more soluble at a low temperature. However, above the crossover pressure region, the solute's vapor pressure becomes
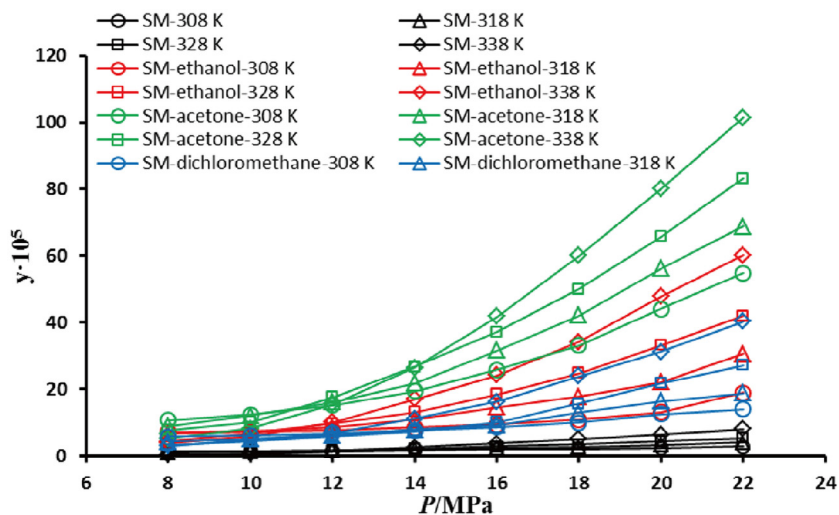

Fig. 4 – Experimental solubility of silymarin in SCCO$_2$ under various conditions with and without a cosolvent.

Table 4 – Correlation parameters for the solubility of silymarin in SCCO$_2$ with and without a cosolvent and AARDs of different semi-empirical models.

Name	Equation[a]	Cosolvent	Correlation parameters			AARD
			A_1	A_2	A_3	
Chrastil	$\ln y = A_1 + A_2 \ln \rho + \dfrac{A_3}{T}$	Without	−5.28	0.81	280.02	10.56%
		Ethanol	13.51	1.94	−7493.37	7.57%
		Acetone	−2.93	1.79	−1671.24	7.57%
		Dichloromethane	7.27	2.36	−6457.65	8.61%
Bartle[b]	$\ln\left(\dfrac{yP}{P_C}\right) = A_1 + A_2(\rho - \rho_C) + \dfrac{A_3}{T}$	Without	48.36	0.011	−13527.69	9.93%
		Ethanol	24.52	0.019	−3053.42	8.89%
		Acetone	21.06	0.005	−4027.82	11.23%
		Dichloromethane	29.48	0.007	−7006.70	8.85%
MST	$T \ln(y\rho) = A_1 + A_2\rho + A_3 T$	Without	−9084.29	2.11	27.27	4.86%
		Ethanol	−9601.20	2.02	30.92	4.58%
		Acetone	−8049.16	2.15	26.61	3.90%
		Dichloromethane	−7323.90	1.74	24.19	4.85%

[a] In this work, values of solubility y are substituted by $y \cdot 10^5$ for convenient operation, without influence on model testing.
[b] P_C and ρ_C are the critical pressure and density of CO_2.

dominant at higher temperature and the density of the solvent turns is less sensitive to the solute's vapor pressure. At the crossover point, these two competitive factors effect rather intense.

Moreover, systems with a cosolvent have greatly increased SM solubility due to the solubility of SM in these organic solvents is much bigger than that in SCCO$_2$. The solubility of SM in different solvents are as follows: acetone > ethanol > dichloromethane. This may be due to the fact SM can form a strong intermolecular hydrogen bonds with acetone and ethanol [35]. Moreover, the polarity of acetone is smaller than that of ethanol, which makes it easier to dissolve SM. All of these make the solubility discrepancy of SM in SCCO$_2$ with different cosolvents

3.2. Correlation results of solubility data

Experimental data were fit with several semi-empirical models as well as BPANN, which enable the prediction of compound solubility in pure SCCO$_2$ and cosolvent-added SCCO$_2$. The correlation results and detailed descriptions of equations are listed in Table 4 and Table 5. The percentage of average absolute relative deviations (AARD%) was applied between the calculated and experimental solubility to study the correlation of the analytes in the models as is mentioned in the following equation:

$$AARD(\%) = \frac{100}{N} \sum_1^N \frac{|y_{cal} - y_{exp}|}{y_{exp}}$$

Table 5 – Correlation parameters for the solubility of silymarin in SCCO$_2$ with and without a cosolvent and AARD of BPANN model.

Name	Cosolvent	AARD
BPANN	Without	1.14%
	Ethanol	1.70%
	Acetone	1.94%
	Dichloromethane	2.15%

where y_{cal} is the calculated value of the mole fraction solubility of solute, y_{exp} is the experimental value of the mole fraction solubility of solutes, and N is the number of experimental points.

As shown in the Table 4 and 5, the AARD% values of the calculated equilibrium solubility for all models are below 11.23%, showing satisfactory accuracy of the experimental results.

Among the semi-empirical models, the MST models provide the minimum AARDs (%) at 4.86, 4.58, 3.90 and 4.85 for SM in pure SCCO$_2$ and in cosolvent-added SCCO$_2$ with ethanol, acetone, and dichloromethane, respectively, indicating a better predictive ability. Fig. 5 compares the calculated isotherms from Chrastil, Bartle, and MST models with the experimental data. As seen, the agreements between the experimental and calculated values are satisfactory and each model agrees well with the experimental data. Moreover, the MST model has a better linear relation, with the plots of $T \ln (y \cdot 10^5 P)$-A_1-$A_2 T$ versus ρ resulting in a nearly straight line.

In this study of BPANN model, it was able to predict the testing subset of solubility by the AARDs (%) of 1.14, 1.70, 1.94, and 2.15 for SM in pure SCCO$_2$ and in cosolvent-added SCCO$_2$ with ethanol, acetone, and dichloromethane, respectively, which are much less than the AARDs of semi-empirical models. After the training, the fitted responses surface was very close to the desired values. For instance, Fig. 6 compares the BPANN predictions to the experimental data via scatter plots for training set of solubility of SM in SCCO$_2$ without cosolvent. The overall performance of training set was evaluated by the determination coefficient (R^2) values ($R^2 = 0.9998$). The proposed model had impressively learned the non-linear relationship between the input and the output variables, exhibiting a successful performance of the BPANN model for prediction of SM solubility in SCCO$_2$ analog in the training stage.

4. Conclusion

In this work, the solubility of silymarin in pure SCCO$_2$ and cosolvent-added SCCO$_2$ was determined at 308, 318, 328
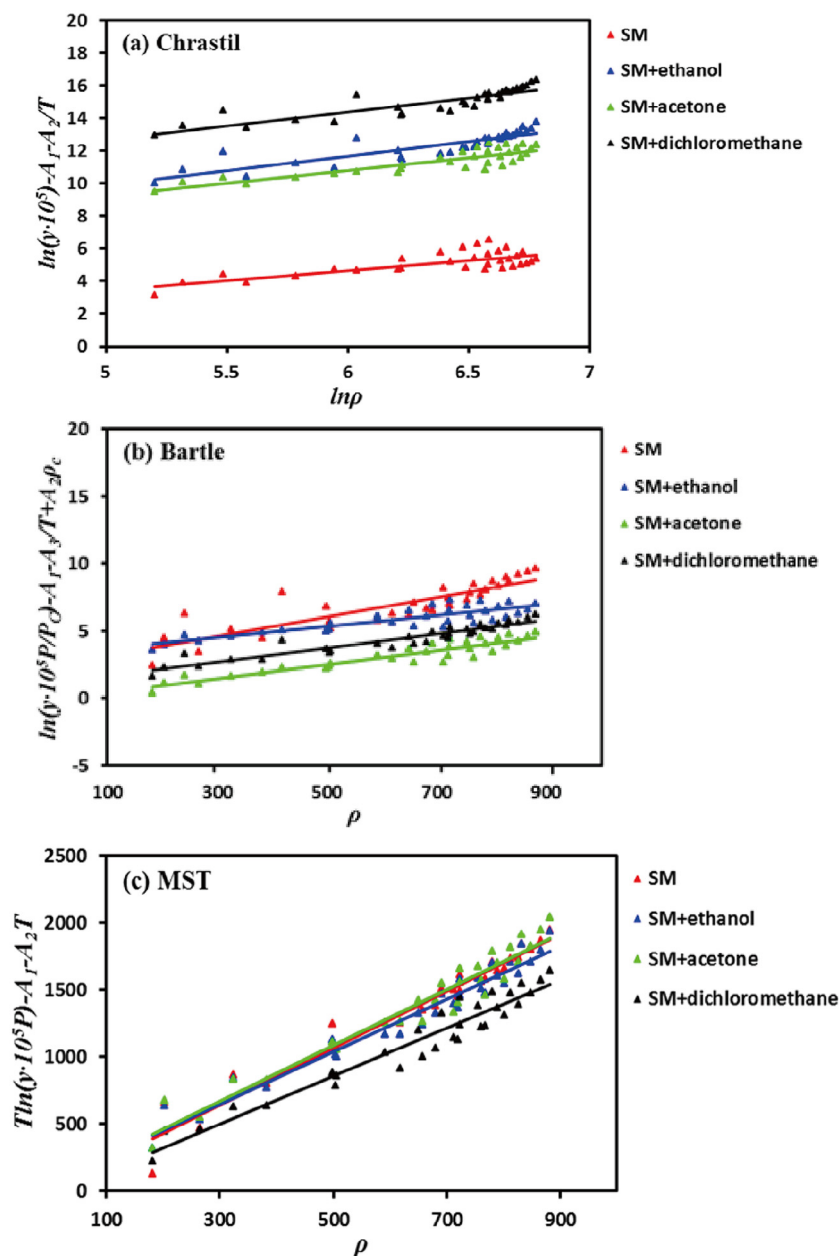
Fig. 5 – Test of consistencies for solubility data of silymarin in SCCO2 with and without a cosolvent using the (a) Chrastil, (b) Bartle, and (c) Mendez-Santiago and Teja (MST) models.

and 338 K, over a pressure range of 8.0 to 22.0 MPa. The solubility of SM ranges from 0.27×10^{-5} to 8.01×10^{-5} in pure SCCO2, 3.89×10^{-5} to 60.12×10^{-5} in ethanol-added SCCO2, 5.17×10^{-5} to 101.37×10^{-5} in acetone-added SCCO2 and 2.99×10^{-5} to 40.33×10^{-5} in dichloromethane-added SCCO2 (at solvent mole fractions of 0.02). Then the experimental solubility data were fit with three semi-empirical models (Chrastil, Bartle and MST models). All fitted models were shown to successfully correlate experimental solubility data with AARDs of 3.90 to 11.23%. Meanwhile, BPANN model was established to fit the solubility data. The BPANN model obtained a more satisfactory accuracy with the AARDs from 1.14 to 2.25% which was lower than those of the other models, suggesting that the BPANN model had a better predictive ability in our study.

Acknowledgments

Conflicts of interest

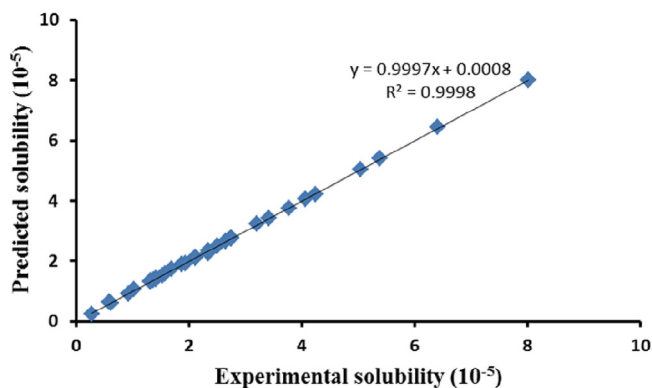The authors declare that there is no conflicts of interest.

Fig. 6 – BPANN predictions (solubility of silymarin in pure SCCO$_2$) and experimental values for training sets.

REFERENCES

[1] Girotra P, Singh SK, Nagpal K. Supercritical fluid technology: a promising approach in pharmaceutical research. Pharm Dev Technol 2013;18:22–38.

[2] Brunner G. Supercritical fluids: technology and application to food processing. J Food Eng 2005;67:21–33.

[3] Reverchon E, Adami R. Nanomaterials and supercritical fluids. J Supercrit Fluids 2006;37:1–22.

[4] Khazaiepoul A, Soleimani M, Salahi S. Solubility prediction of disperse dyes in supercritical carbon dioxide and ethanol as co-solvent using neural network. Chin J Chem Eng 2016;24:491–498.

[5] Zuknik MH, Norulaini NAN, Omar AKM. Supercritical carbon dioxide extraction of lycopene: a review. J Food Eng 2012;112:253–262.

[6] Sahena F, Zaidul ISM, Jinap S. Application of supercritical CO$_2$ in lipid extraction – A review. J Food Eng 2009;95:240–253.

[7] Park MW, Bae HK. Dye distribution in supercritical dyeing with carbon dioxide. J. Supercritical Fluid. 2002;22:65–73.

[8] Byrappa K, Ohara S, Adschiri T. Nanoparticles synthesis using supercritical fluid technology-towards biomedical applications. Adv Drug Deliv Rev 2008;60:299–327.

[9] Shen BQ, Feng LF, Li SF, et al. Correlating and predicting the solubilities of polycyclic aromatic hydrocarbons in supercritical fluids using the compressed gas model and the reference solubilities. Fluid Phase Equilib 2013;337:100–108.

[10] Wu H, Zhu J, Wang YW, et al. Measurement and modeling for solubility of 3-hydroxybenzaldehyde and its mixture with 4-hydroxybenzaldehyde in supercritical carbon dioxide. Fluid Phase Equilib 2016;409:271–279.

[11] Peng J, Yang HJ, Yang HW. Solubilities and partial molar volumes of three bis (2-ethoxyethyl) ethanedioate derivatives in supercritical carbon dioxide. J Chem Thermodyn 2015;83:33–42.

[12] Li HR, Jia DD, Liu RH, et al. Correlating and estimating the solubilities of solid organic compounds in supercritical CO$_2$ based on the modified expanded liquid model and the group contribution method. Fluid Phase Equilibr. 2014;385:10–24.

[13] Lamba N, Narayan RC, Modak J, et al. Solubilities of 10-undecenoic acid and geraniol in supercritical carbon dioxide. J Supercrit Fluids 2015;107:384–391.

[14] Asiabi H, Yamini Y, Latifeh F, et al. Solubilities of four macrolide antibiotics in supercritical carbon dioxide and their correlations using semi-empirical models. J Supercrit Fluids 2015;104:62–69.

[15] Sato M, Takeda K, Ota M, et al. Solubility estimation of high-value natural products in supercritical CO$_2$ based on solubility parameter. Kagaku Kogaku Ronbun 2010;36:466–471.

[16] Kiyoshi M, Kenji M, Ryugen O, et al. Solubilities of 7, 8-dihydroxyflavone and 3, 3', 4', 5, 7 pentahydroxyflavone in supercritical carbon dioxide. J Chem Eng Data 2003;48:1040–1043.

[17] Dixit N, Baboota S, Kohli K, et al. Silymarin: a review of pharmacological aspects and bioavailability enhancement approaches. Indian J Pharmacol 2007;39:172–179.

[18] Campodónico A, Collado E, Ricci R, et al. Dissolution test for silymarin tablets and capsules. Drug Dev Ind Pharm 2001;27:261–265.

[19] Tedesco D, Tava A, Galletti S, et al. Effects of silymarin, a natural hepatoprotector, in periparturient dairy cows. J Dairy Sci 2004;87:2239–2247.

[20] Shaker ME, Shiha GE, Ibrahim TM. Comparison of early treatment with low doses of nilotinib, imatinib and a clinically relevant dose of silymarin in thioacetamide-induced liver fibrosis. Eur J Pharmacol 2011;670:593–600.

[21] Kvasnička F, BıBa B, ŠevčıK R, et al. Analysis of the active components of silymarin. J Chromatogr A 2003;990:239–245.

[22] Honjo M, Mishima K, Matsuyama K, et al. Extraction of silymarins from milk thistle seeds using supercritical carbon dioxide with methanol. Solvent Extraction Res. Dev. 2009;16:111–120.

[23] Çelik HT, Gürü M. Extraction of oil and silybin compounds from milk thistle seeds using supercritical carbon dioxide. J. Supercritical Fluid 2015;100:105–109.

[24] Yang G, Zhao YP, Feng NP. Preparation and in vitro release of silymarin nanoparticles by supercritical anti-solvent. Chin. Pharm. J. 2015;50:784–788.

[25] Yang G, Zhao YP, Feng NP, et al. Improved dissolution and bioavailability of silymarin delivered by a solid dispersion prepared using supercritical fluids. Asian J Pharm Sci 2015;10:194–202.

[26] Yang G, Zhao YP, Zhang Y, et al. Enhanced oral bioavailability of silymarin using liposomes containing a bile salt: preparation by supercritical fluid technology and evaluation in vitro and in vivo. Int J Nanomedicine 2015;10:1–12.

[27] Chrastil J. Solubility of solids and liquids in supercritical gases. J Phys Chem C 1982;86:3016–3021.

[28] Bartle KD, Clifford AA, Jafar SA. Solubilities of solids and liquids of low volatility in supercritical carbon dioxide. J Phys Chem Ref Data 1991;20:713–756.

[29] Méndez-Santiago J, Teja AS. The solubility of solids in supercritical fluids. Fluid Phase Equilibr. 1999;158–160:501–510.

[30] Medina I, Bueno JL. Solubilities of 2-nitroanisole and 3-phenyl-1-propanol in supercritical carbon dioxide. J Chem Eng Data 2000;45:298–300.

[31] Su CS, Chen YP. Correlation for the solubilities of pharmaceutical compounds in supercritical carbon dioxide. Fluid Phase Equilib 2007;254:167–173.

[32] Rohani AA, Pazuki G, Najafabadi HA. Comparison between the artificial neural network system and SAFT equation in obtaining vapor pressure and liquid density of pure alcohols. Expert Syst. Appl. 2011;38:1738–1747.

[33] Li SM, Liu Y, Liu T, et al. Development and in-vivo assessment of the bioavailability of oridonin solid dispersions by the gas anti-solvent technique. Int J Pharm 2011;411:172–177.

[34] Jin JS, Ning YY, Hu K, et al. Solubility of p-nitroaniline in supercritical carbon dioxide with and without mixed cosolvents. J Chem Eng Data 2013;58:1464–1469.

[35] Jia JF, Zabihi F, Gao YH, et al. Solubility of glycyrrhizin in supercritical carbon dioxide with and without cosolvent. J Chem Eng Data 2015;60:1744–1749.